Designing a Model for the Enzyme–Substrate Complex to Investigate the Detailed Catalytic Mechanism of Lactoperoxidase by Quantum Chemical Methods

Brandon Manary, Jorge Llano*

Department of Physical Sciences, MacEwan University, PO Box 1796, Alberta T5J 2P2, Canada

Introduction

LACTOPEROXIDASE (LPO) is a heme enzyme found in exocrine secretions such as milk, saliva and endodermal mucus. LPO catalyzes the formation of oxidizing oxoanions that act as natural antibiotics in those body fluids. LPO is a versatile enzyme that converts thiocyanate ions (SCN^-) to hypothiocyanite ions ($OSCN^-$), as well as halide ions (i.e., Cl^-, Br^- and I^-) to hypohalite ions (i.e., ClO^-, BrO^- and IO^-). These highly oxidizing agents are toxic to germs such as oral streptococci,[1] *Porphyromonas gingivalis*,[2] *Helicobacter pylori*,[3] *Salmonella typhimurium*, HIV, herpes simplex type 1, and the influenza virus.[4,5]

LPO belongs to the peroxidase family of enzymes, which also includes myeloperoxidase (MPO), eosinophil peroxidase (EPO) and thyroid peroxidase (TPO). LPO, MPO and EPO protect organisms against microbial infections as part of their innate immune system. MPO and EPO are stored in the granules of white blood cells, whereas LPO is steadily released in the mucus lining of airways, as well as in saliva, tears and milk.[6] In particular, TPO is involved in the synthesis of thyroid hormones.

Table 1. Concentrations of SCN^- and HOSCN Present in Biological Fluids.[6]

Fluid	[SCN^-]	[HOSCN]
Plasma	(10 to 100) μM	N/A
Saliva	(0.3 to 3) mM	(10 to 60) μM
Lung bronchioalveolar fluid	≤ 500 μM	N/A
Upper airway (nasal) ASL fluid	400 μM	N/A

As other peroxidase enzymes, LPO and MPO use H_2O_2 to convert its substrates into potent oxidizing agents, according to the following **catalytic cycle**:[7,8,9,10]

STAGE 1. Enzyme activation:

$$\text{Enz–Fe}^{3+} \xrightarrow{H_2O_2 \;\; H_2O} \text{Enz–Fe}^{3+}\text{–O}^{\bullet} \leftrightarrow \text{Enz–Fe}^{\bullet 4+}\text{=O}$$

Ground-state → Compound I

STAGE 2. Two-electron oxidation of a (pseudo)halide:

$$\text{Enz–Fe}^{3+}\text{–O}^{\bullet} \leftrightarrow \text{Enz–Fe}^{\bullet 4+}\text{=O} \xrightarrow{X^- \;\; XO^-} \text{Enz–Fe}^{3+} \quad (X = NCS, Cl, Br, I)$$

Compound I → Ground-state

Results

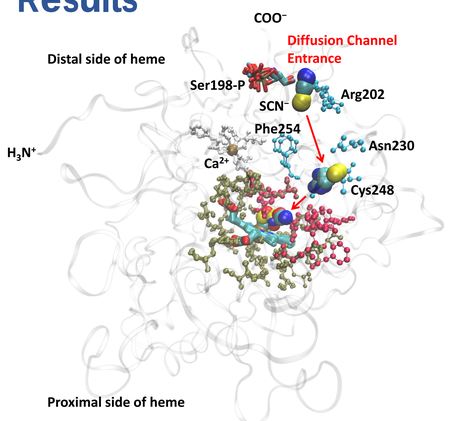

Figure 1. The path (→) of substrate molecules along the diffusion channel found by an RMSD overlapping of the LPO crystallographic structures.

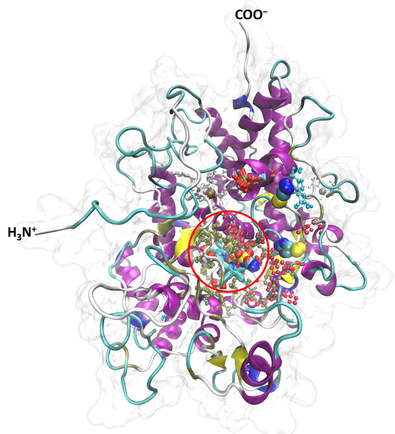

Figure 2. Representation of LPO's tertiary structure with superimposed active-sites embedded. The active sites (circled) of all the crystallographic structures were overlapped and centered on the heme group.

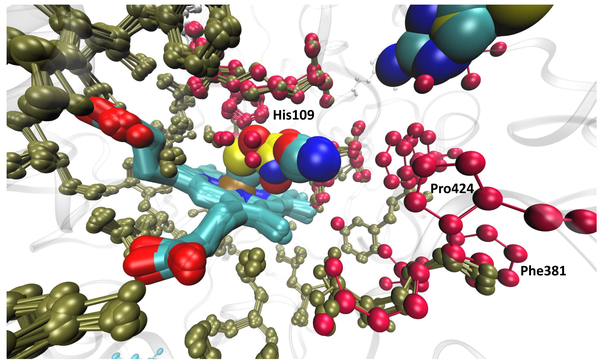

Figure 3. Representation of the active sites of all the LPO structures overlapped and centered on the heme group.

- Glu257, Gln258, Gln104, Arg255, His109 located over the distal side of the heme do not show significant conformational flexibility in all the aligned iron-complexed structures.
- Phe381 and Pro424 are conformationally flexible because they belong structurally to the diffusion channel of the enzyme.

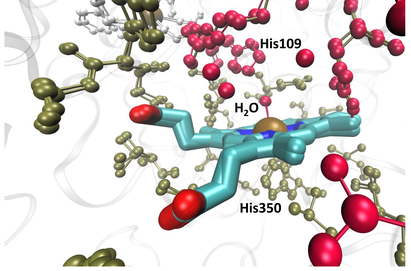

Figure 4. The ground-state of the enzyme with water bound to iron in the active site (PDB: 2PT3, 3GCL).

- His109 is hydrogen-bonded to a water molecule, and the water molecule is ligated to the iron center.

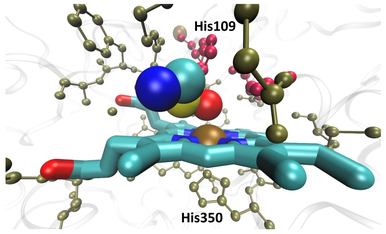

Figure 5. Intermediate structure (PDB: 3BXI) that precedes the enzyme–product complex in the reaction mechanism.

- The oxygen of $OSCN^-$ is bound directly to the iron atom.

Conclusions

- The catalytic functional groups (i.e., Glu257, Gln258, Gln104, Arg255, His109) located on the distal side of these enzymes form a network that hinders their side-chain conformational flexibility, regardless of the bulkiness of the ligand docked in the active site.
- All the residues within a distance of approximately 15 Å from the iron center will be included in the chemical model of the active site that will be used to compute the detailed catalytic mechanism of LPO and MPO by quantum chemical methods.

Figure 6. Multiple sequence alignment of LPO chains indicates that the secondary and tertiary structures are conserved (PDB: 3BXI, 3FAQ, 3ERI, 3NYH, 3V6Q, 3TGY, 3Q9K, 2PT3 3GCL, 2QRB, 2IPS, 2OJV).

Methods

The crystallographic structures for LPO and MPO enzymes were retrieved from the Protein Data Bank (PDB) to visualize and assess the conformational flexibility of the active-site functional groups in the available protein structures complexed with ligands of variable bulkiness.

The geometrical configurations of the active site were compared by an RMSD alignment of the structures centered on the prosthetic heme group of the enzymes.

Visualization of structures and multiple sequence alignments using the STAMP algorithm were performed with the VMD software.[17]

Table 2. Description of the Crystallographic Structures of LPO and MPO Examined in this Work. →

PDB Accession Code	Resolution	Iron-bound Ligand	Ligand-bound Species	Taxonomy	Reference
3BXI (LPO)	2.3 Å	$NCSO^-$		*Bos taurus*	11
3FAQ (LPO)	2.7 Å	CN^-	$NCSO^-$	*Bubalus bubalis*	12
3ERI (LPO)	2.5 Å	SCN^-		*Bos taurus*	13
3NYH (LPO)	1.77 Å	Br^-		*Bos taurus*	14
3V6Q (LPO)	2.0 Å	CO	Br^-	*Bos taurus*	PDB, 2011
3TGY (LPO)	2.35 Å	H_2Asc (ascorbic acid)		*Bos taurus*	PDB, 2011
3Q9K (LPO)	1.7 Å	C_6H_5–NH–HC=S (methanethioamide)		*Bos taurus*	PDB, 2011
2PT3 (LPO)	2.34 Å	H_2O	PO_4^{3-}	*Bos taurus*	PDB, 2007
3GCL (LPO)	2.5 Å	H_2O	ASA	*Bos taurus*	PDB, 2009
2QRB (LPO)	2.5 Å	Cl^-		*Bos taurus*	PDB, 2007
2IPS (LPO)	3.1 Å	SCN^-		*Bos taurus*	PDB, 2006
3NAK (LPO)	3.3 Å			*Capra hircus*	PDB, 2010
3N8F (LPO)	3.25 Å			*Capra hircus*	PDB, 2010
2OJV (LPO)	2.4 Å	CN^-	I^-	*Capra hircus*	PDB, 2007
1D7W (MPO)	1.9 Å			*Homo sapiens*	15
1DNW (MPO)	1.9 Å			*Homo sapiens*	15
1CXP (MPO)	1.8 Å			*Homo sapiens*	16

References

(1) Thomas, E. L.; Milligan, T. W.; Joyner, R. E.; Jefferson, M. M. *Infect. Immun.* **1994**, *62*, 529.
(2) Shin, K.; Horigome, A.; Wakabayashi, H.; Yamauchi, K.; Yaeshima, T.; Iwatsuki, K. *J. Breath Res.* **2008**, *2*, 017014.
(3) Haukioja, A.; Ihalin, R.; Loimaranta, V.; Lenander, M.; Tenovuo, J. *J. Med. Microbiol.* **2004**, *53*, 855.
(4) Tenovuo, J. *J. Dent. Res.* **2002**, *81*, 807.
(5) Cegolon, L.; Salata, C.; Piccoli, E.; Juarez, V.; Palu, G.; Mastrangelo, G.; Calistri, A. *Int. J. Hyg. Environ. Health* **2014**, *217*, 17.
(6) Barrett, T. J.; Hawkins, C. L. *Chem. Res. in Toxicol.* **2012**, *25*, 263.
(7) Flemmig, J.; Remmler, J.; Rohring, F.; Arnhold, J. *J. Inorg. Biochem.* **2014**, *130*, 84.
(8) Bafort, F.; Parisi, O.; Perraudin, J. P.; Jijakli, M. H. *Enzyme Res.* **2014**, *2014*, 517164.
(9) Furtmuller, P. G.; Arnhold, J.; Jantschko, W.; Zederbauer, M.; Jakopitsch, C.; Obinger, C. *J. Inorg. Biochem.* **2005**, *99*, 1220.
(10) Davies, M. J. *J. Clin. Biochem. Nutr.* **2011**, *48*, 8.
(11) Singh, A. K.; Singh, N.; Sharma, S.; Shin, K.; Takase, M.; Kaur, P.; Srinivasan, A.; Singh, T. P. *Biophys. J.* **2009**, *96*, 646.
(12) Sheikh, I. A.; Singh, A. K.; Singh, N.; Sinha, M.; Singh, S. B.; Bhushan, A.; Kaur, P.; Srinivasan, A.; Sharma, S.; Singh, T. P. *J. Biol. Chem.* **2009**, *284*, 14849.
(13) Singh, A. K.; Singh, N.; Sinha, M.; Bhushan, A.; Kaur, P.; Srinivasan, A.; Sharma, S.; Singh, T. P. *J. Biol. Chem.* **2009**, *284*, 20311.
(14) Singh, A. K.; Pandey, N.; Sinha, M.; Kaur, P.; Sharma, S.; Singh, T. P. *Int. J. Biochem. Mol. Biol.* **2011**, *2*, 328.
(15) Blair-Johnson, M.; Fiedler, T.; Fenna, R. *Biochem.* **2001**, *40*, 13990.
(16) Fiedler, T. J.; Davey, C. A.; Fenna, R. E. *J. Biol. Chem.* **2000**, *275*, 11964.
(17) http://www.ks.uiuc.edu/Research/vmd/